Available online at www.sciencedirect.com

ScienceDirect

IFAC Papers Online CONFERENCE PAPER ARCHIVE

IFAC PapersOnLine 58-20 (2024) 380–385

Exploiting Fano resonance in wave energy systems ⋆

Andrei M. Ermakov * **Jack L. Rose-Butcher** **
Yury A. Stepanyants *** **John V. Ringwood** ****

* *Centre for Ocean Energy Research, Maynooth University, Co. Kildare, Ireland (e-mail: andrei.ermakov@mu.ie)*
** *Hanze University of Applied Sciences, Groningen, Netherlands (e-mail: j.l.rose-butcher@st.hanze.nl)*
*** *School of Science, University of Southern Queensland, Toowoomba, Queensland, Australia (e-mail: yury.stepanyants@usq.edu.au)*
**** *Centre for Ocean Energy Research, Maynooth University, Co. Kildare, Ireland (e-mail: john.ringwood@mu.ie*

Abstract: Energy maximising control of wave energy converters (WECs) typically results in exaggerated motion of the device, with consequent increases in mooring and other forces which can adversely affect WEC lifetime. In addition, the exaggerated motion typically increases the incidence of nonlinear hydrodynamic effects, confounding linear analysis upon which many WEC control design paradigms are based. This paper explores the potential to exploit Fano resonance in a wave energy context, where the WEC body remains relatively stationary, while the active power take-off elements are well exercised. Preliminary results suggest that significant WEC body motion reduction is possible, with a modest reduction in energy capture.

Keywords: Wave energy converter, Fano resonance, control

1. INTRODUCTION

Fano resonance can be observed in a number of application areas, but perhaps best illustrated in the well-known executive toy illustrated in Fig/1. In essence, part of the

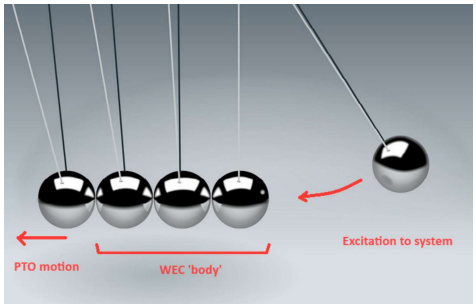

Fig. 1. A classic example of Fano resonance, with extension to the WEC case.

'system', excited by an external force, remains relatively stationary, while the excitation energy is transmitted to another part of the system which is free to move. In the wave energy case, the external excitation is provided by hydrodynamic wave forces, the relatively stationary part can be the WEC hull, while the moving part is the power take-off (PTO) which ultimately converts the wave energy into a useable form.

The Fano resonance effect, known also as dynamic damping, can also be explained in terms of two pendulums connected by a spring (Rabinovich and Trubetskov, 1989; Tribelsky, 2014). While the first pendulum influenced by a periodic excitation may be relatively immovable, or oscillates with a small amplitude at a certain frequency, the second one can experience large-amplitude oscillations at the same frequency. This mechanism is also very similar to the operational principle of a tuned mass damper, which can prevent damage or outright structural failure, and is commonly used in power transmission, automobiles, and buildings (Lee et al., 2006).

In the wave energy application, it is well known that (for resonating devices) the addition of energy maximising control results in exaggerated motion (Windt et al., 2021), often with some undesirable side effects, including an increase in mooring forces and significantly more fatigue and system wear. The objective, in this paper, is to examine Fano resonance as a tool to provide a better balance between energy maximisation and WEC hull motion. To that end, we examine a device with the structure as shown in Fig.2, where the complete PTO system is internal to the WEC hull. The internal mass moves somewhat independently of the hull, which are connected by a linear generator (LinGen, converting the useful energy) and an

⋆ This work was supported by Science Foundation Ireland under Grant number 20/US/3687 and supported in part by a research grant from Science Foundation Ireland and the Sustainable Energy Authority of Ireland under SFI-IRC Pathway Programme 22/PATH-S/10793 and SFI Frontiers Grant 21/FFP-A/8997; Y.S. acknowledges the funding provided by grant No. FSWE-2023-0004 through the State task program in the sphere of scientific activity of the RF Ministry of Science and Higher Education and grant No. NSH-70.2022.1.5 provided by the President Council of the Russian Federation for the State support of leading Scientific Schools of the Russian Federation.

10.1016/j.ifacol.2024.10.083

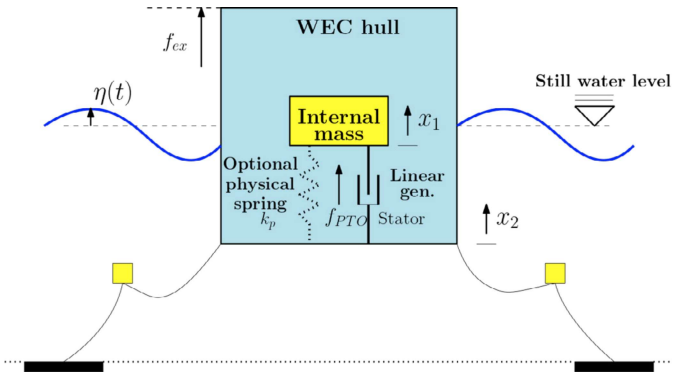

Fig. 2. 2-body loosely moored WEC with oscillating internal mass.

optional physical spring. Note that the LinGen could also provide a virtual spring effect, though it may be more economical to use a physical spring. The arrangement in Fig.2 has some similarities with the Vibro-Impact device reported in Guo and Ringwood (2021), but with less exotic dynamics, due to the absence of a spring air gap.

Specifically, this paper addressed two terms which contribute to levelised cost of energy (LCoE):

$$LCoE = \frac{CapEx + OpEx}{EP}. \tag{1}$$

where $CapEx$ and $OpEx$ denote capital and operational expenditure, respectively, while EP represents energy produced. While most studies related to WEC control target only EP (Ringwood et al., 2023), this paper also targets $OpEx$, which relates to maintenance requirements and device degradation, which can be related to device motion variance. We assume that capital costs are independent of control actions.

The remainder of the paper is laid out as follows: Section 2 develops the mathematical model of the system, while Section 3 outlines the control calculations to modulate the level for Fano resonance. Sections 4 introduces a reference single-body device. Sections 5, 6 and 7 document some sample results, and draw some conclusions.

2. MATHEMATICAL MODEL

The present study addresses a one degree-of-freedom problem, limiting displacements to the heave direction. The heaving buoy WEC position in waves is traditionally modelled by Cummins' equation (Cummins, 1962):

$$(m_h + m_\infty)\,\ddot{x}_2(t) + \int_0^t \dot{x}_2(\tau) k_r(t-\tau) d\tau + d_h \dot{x}_2(t) + k_s x_2(t) = f_{ex}(t) + f_{PTO}(t), \tag{2}$$

where $x_2(t)$ represents the vertical position of the buoy, m_h is the mass of the buoy hull (which also includes the LinGen stator), and m_∞ denotes the added-mass at infinite frequency, $k_r(t)$ is the radiation damping impulse response function, k_s is the hydrostatic stiffness, d_h the (linearised) viscous water damping, $f_{ex}(t)$ the wave excitation force, and $f_{PTO}(t)$ describes the force applied by the PTO system.

In terms of the internal system dynamics, the position $x_1(t)$ of the LinGen translator can be described by:

$$m_p \ddot{x}_1(t) = -f_{PTO}, \tag{3}$$

and

$$f_{PTO} = f_{gen} + k_p[x_1(t) - x_2(t)], \tag{4}$$

where m_p represents the internal system mass of the LinGen translator and internal mass, k_p is the stiffness of the (optional) physical spring, and f_{gen} is the force generated by the linear generator.

3. CONTROL CALCULATIONS

We can choose f_{gen} to have the following components:

$$f_{gen}(t) = k_c\,[x_1(t) - x_2(t)] + d_c\,[\dot{x}_1(t) - \dot{x}_2(t)] + m_c\,[\ddot{x}_1(t) - \ddot{x}_2(t)], \tag{5}$$

where m_c and k_c are virtual mass and spring parameters respectively, and d_c is the damping parameter, which converts useful energy.

As a result, the complete dynamics of the internal system (from (3)) are:

$$m_p\,\ddot{x}_1(t) = (k_p + k_c)[\,x_2(t) - x_1(t)] + d_c\,[\dot{x}_2(t) - \dot{x}_1(t)] + m_c\,[\ddot{x}_2(t) - \ddot{x}_1(t)]. \tag{6}$$

Equation (6) while allowing for full complex-conjugate control (Ringwood et al., 2023) of the system for monochromatic waves, contains some redundancy, due to the provision of both inertia and spring terms. This allows for some flexibility in terms of:

- Frequency response shaping (e.g. it has been shown that the use of an inertial term can give a broader frequency response (Hansen, 2013)), and
- The spring and inertial terms due to the LinGen control force (i.e. k_c and m_c) are complemented by the physical terms due to m_p and k_p.

The final decision as to how to balance m_p, k_p, m_c and k_c is based on economic considerations related to a minimum cost solution. However, it should be borne in mind that even though it may be cheaper to utilise predominantly physical mass and spring than implement through f_{gen}, the virtual quantities can be continuously adapted to cater for, for example, sea state changes.

The solution to the system described by equations (2)–(6) can be determined in the frequency domain, under the following assumptions:

$$x_1(t) = X_1(\omega)e^{j\omega t}, \qquad x_2(t) = X_2(\omega)e^{j\omega t}, \tag{7}$$

$$f_{ex}(t) = F_{ex}(\omega)e^{j\omega t}, \tag{8}$$

where $X_1(\omega)$ and $X_2(\omega)$ denote the response amplitude operators (RAO) for the heaving buoy and translator, respectively, and $F_{ex}(\omega)$ represents the excitation force to wave frequency response.

The solution to Cummins equation (2) for a body in waves can be obtained in the frequency domain using a boundary element method (BEM) based software such

as Ansys AQWA (2015). The obtained solutions for the heaving buoy hull displacement $X_2(\omega)$ for each particular frequency of a regular wave can be expressed in terms of the intrinsic system impedance, $Z(\omega)$ (Falnes, 2002) as:

$$X_2(\omega) = \frac{F_{ex}(\omega) + F_{PTO}(\omega)}{j\omega Z_{hull}}(\omega), \tag{9}$$

where

$$F_{PTO}(\omega) = [(k_c + k_p) + j\omega d_c \ -\omega^2 m_c] \cdot(X_1(\omega) - X_2(\omega)), \tag{10}$$

and we can identify:

$$Z_{pto} = [(k_c + k_p) + j\omega d_c - \omega^2 m_c]/(j\omega) \tag{11}$$

as the intrinsic impedance referred to the PTO, and it is clear that the imaginary part of Z_{pto} can be manipulated by either k_c, k_p, or m_c.

The intrinsic impedance of the system, referred to the WEC hull, Z_{hull} is:

$$Z_{hull}(\omega) = B(\omega) + j\omega \left[m_h + M_a(\omega) + m_\infty - \frac{k_s}{\omega^2} \right], \tag{12}$$

where $B(\omega)$ is the radiation resistance, $M_a(\omega)$ is the added mass after the singularity at infinite frequency M_∞ is removed.

The RAO of the heaving buoy hull $X_0(\omega)$, free from any PTO forces, can be determined as:

$$X_0(\omega) = \frac{F_{ex}(\omega)}{j\omega Z_{hull}(\omega)}. \tag{13}$$

The equation for the position RAO of the translator (3) in the frequency domain takes the following form:

$$m_p\, \omega^2 X_1(\omega) = F_{PTO}(\omega). \tag{14}$$

Then, in the frequency domain, the solution to the system described by equations (9), (10) and (14), for the RAOs of the buoy and the translator, respectively, is given by:

$$X_1(\omega) = \frac{F_{ex}(\omega)}{\Delta}[k_p + (k_c + j\,\omega\, d_c - m_c\,\omega^2)], \tag{15}$$

$$X_2(\omega) = \frac{F_{ex}(\omega)}{\Delta}[(k_p - \ m_p\,\omega^2) + (k_c + j\,d_c\,\omega - m_c\,\omega^2)], \tag{16}$$

where

$$\Delta = j\omega\ Z_{hull}(\omega)[(k_p - m_p\,\omega^2) + (k_c + j\,d_c\,\omega - m_c\,\omega^2)] - m_p\,\omega^2[k_p + (k_c + j\,\omega\,d_c - m_c\,\omega^2)]. \tag{17}$$

The time-averaged power, produced by the linear generator of the described system in regular waves, can be calculated as:

$$P(\omega) = d_c\,|V_1(\omega) - V_2(\omega)|^2/2, \tag{18}$$

where $V_1(\omega) = j\omega X_1(\omega)$ is the velocity RAO of the translator, and $V_2(\omega) = j\omega X_2(\omega)$ is the velocity RAO of the heaving buoy.

A rough estimate of the average power generation P_{avr} for a specific sea state can be determined by integrating the product of the average power generation for a given wave frequency $P(\omega)$, and the probability distribution function for the frequencies of that sea state $p_{ss}(\omega)$ across all wave frequencies:

$$P_{avr} = \int_0^\infty P(\omega)\, p_{ss}(\omega)\, d\omega, \tag{19}$$

and can be extended to a complete wave climate using a scatter plot, showing the set of probabilities for all occurring sea states in a specific location. Note that:

$$\int_0^\infty p_{ss}(\omega) d\omega = 1. \tag{20}$$

4. REFERENCE SINGLE-BODY DEVICE

To assess the effectiveness of the 2-body loosely-moored WEC with oscillating internal mass, and to determine whether a heaving buoy hull should be considered primarily as a *source* or *transmitter* of energy for the PTO system, the authors compare the time-averaged power production of the internal PTO (as illustrated in Fig. 2) with that of the PTO for a more traditional bottom-referenced point absorber (shown in Fig. 3). The hull shape of the buoy is identical for both devices. The study assumes that the ocean bed-referenced PTO operates under a 'simple and effective' (S+E) complex-conjugate controller (Fusco and Ringwood, 2013), which can be similar in form to the f_{gen} parameterisation in (5).

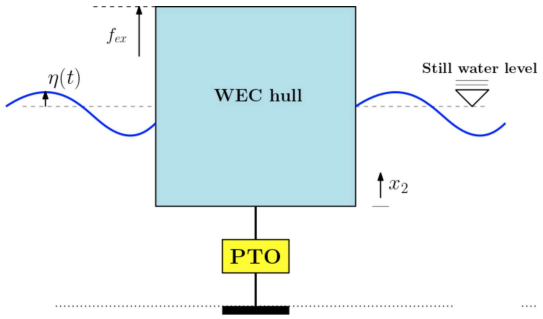

Fig. 3. A single body WEC with an ocean bed referenced PTO system.

In the S+E control method, applied to the ocean bed-referenced WEC, the intrinsic impedance of the PTO system $Z^*_{pto}(\omega)$ is determined by the following equation:

$$Z^*_{pto}(\omega) = (2\alpha - 1)Re[Z_{hull}(\omega)] - j\,Im[Z_{hull}(\omega)], \tag{21}$$

where α represents a PTO damping tuning parameter, used to impose a constraints on the device displacement. However, when $\alpha = 1$, the traditional (unconstrained) complex conjugate control solution is obtained.

The corresponding RAOs for displacement $X_2(\omega)$ and velocity $V_2(\omega)$, for the ocean bed-referenced WEC buoy hull, can be respectively determined using:

$$X_2(\omega) = V_2(\omega)/(j\,\omega), \tag{22}$$

with

$$V_2(\omega) = \frac{F_{ex}(\omega)}{Z_{hull}(\omega) + Z^*_{pto}(\omega)} = \frac{F_{ex}(\omega)}{2\,\alpha\, Re[Z_{hull}(\omega)]}. \tag{23}$$

It is evident that an increase in the damping parameter α results in a decrease in both the magnitude *and* velocity of the buoy. The parameter α can be determined based on a maximum magnitude constraint $|X_2| < X_2^{Max}$.

The maximum time averaged power production $\tilde{P}(\omega)$ in the frequency domain (Falnes, 2002) due to the constrained magnitude $|X_2(\omega)|$ can be evaluated as

$$\tilde{P}(\omega) = \frac{1}{2} Re[Z^*_{pto}(\omega)]|V_2(\omega)|^2 = \frac{(2\alpha - 1)|F_{ex}(\omega)|^2}{8\,\alpha^2\, Re[Z_{hull}(\omega)]}. \quad (24)$$

5. SAMPLE RESULTS

5.1 Example 1

This example focuses on determining the optimal operational regime and the required Z_{PTO} parameters for a self-contained WEC system (Fig. 2). This optimization aims to maximize power generation P (18) while limiting the maximum buoy hull magnitude $|X_2|$ (16). The optimization is carried out for regular waves with various frequencies $0 < \omega < 3$ rad/s and wave height H=1 m, so that the frequency-specific behaviour of the system can be studied. The selected buoy hull is a cylinder with a radius r=2 m, height h=4 m, and mass m_h=19,132 kg. The chosen internal mass is m_p=6,377 kg, leading to a semi-submerged state for the buoy hull in still water. The corresponding intrinsic impedance, $Z_{hull}(\omega)$, and excitation force $F_{ex}(\omega)$ frequency responses are computed in (Ansys AQWA, 2015) and then interpolated using a high-order polynomial in ω (see Fig. 4).

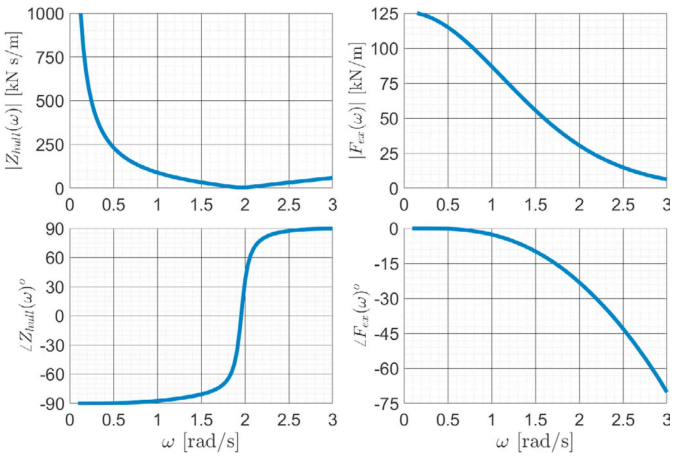

Fig. 4. Intrinsic impedance Z and excitation force F_{ex} frequency responses for a semi-submerged cylindrical buoy hull with dimensions: r=2m, h=4m, and mass m_h=19,132kg, computed using Ansys AQWA (2015).

While the objective is to maximize power generation (18) by optimising the PTO parameters Z_{PTO}, it is desired that the displacement of the heaving buoy hull remains relatively small e.g. $|X_2| < 1$ m. Additionally, the relative magnitude of the translator is restricted by the buoy hull height, but remains adequate for power generation $0.25 < |X_1 - X_2| < 2$ m. The position constraints are enforced by optimizing the Z_{pto} response as per eqs. (15) and (16).

Therefore, a constrained optimization problem, expressed in the following form, is solved:

$$P(\omega) \rightarrow Max,$$
$$|X_2| < 1m, \quad 0.25 < |X_1 - X_2| < 2m. \quad (25)$$

The solution to optimisation problem (25) is illustrated in Fig. 5. It is visible, in Fig. 5a, that the buoy hull magnitude constraints (blue line) are active until ω >2.2 rad/s. The translator (red line) predominantly operates at the upper limit of its allowed magnitude, with an exception near the hull resonant frequency (yellow line), at ω=1.9 rad/s, where maximum energy extraction is achieved, with P=30 kW (see. Fig. 5d). This magnitude reduction aligns with the rapid increase, and drop, of the Z_{PTO} parameters as illustrated in Fig. 5c. Fig. 5b shows that the translator and buoy hull are 90° out of phase while, for $\omega < 1.9$ rad/s), the fluctuations shift to being in-phase.

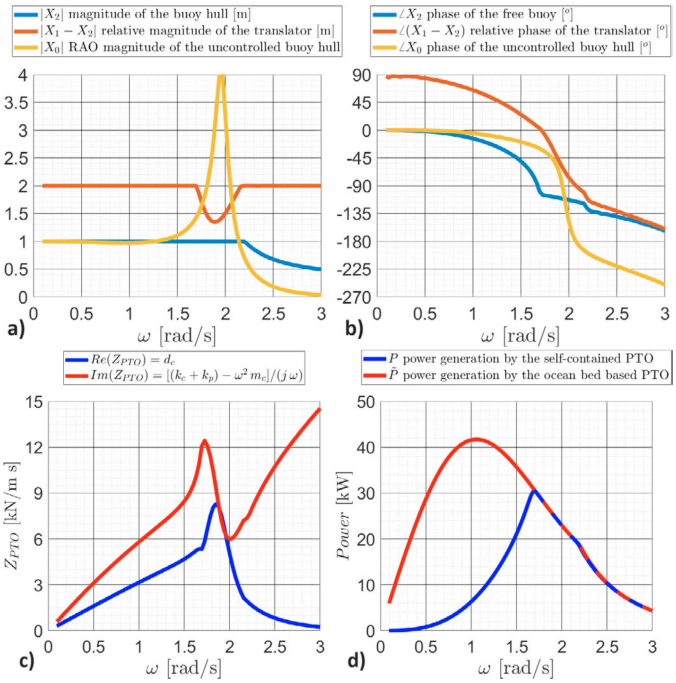

Fig. 5. Optimal constrained control solution for the 2-body semi-submerged cylindrical buoy hull with dimensions: r=2m, h=4m, and mass m_h=19,132kg; a) Magnitudes for the buoy hull and internal translator; b) Corresponding phases; c) Optimal PTO parameters Z_{PTO}; d) Comparison of power generation between the self-contained blue line) and ocean bed-referenced (red line) PTO systems , operating under the same buoy hull magnitude constraints (Fig. (a) blue line).

A comparison of the power generation by a 2-body self-contained (Fig. 2) and the reference ocean bed-based (Fig. 3) systems, operating under the same buoy hull magnitude constraint, is shown in Fig. 5d. It is clear that the ocean bed-referenced PTO can generate more power when $\omega < 1.7$ rad/s. However, the ocean bed-referenced PTO would require a significant reactive force, causing substantial loading on the mooring structure.

From Fig. 5d, it is also visible that, when $\omega > 1.7$ rad/s, the self-contained system has similar performance to the

ocean bed-referenced PTO system, utilizing damping control and adhering to the same magnitude $|X_2|$ constraint. This implies that optimum power transmission has been parametrically achieved, with the heaving buoy hull functioning as a transmitter of wave energy while resonance is realized within the internal PTO system.

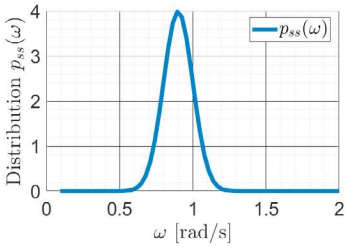

Fig. 6. Wave frequency distribution $p_{ss}(\omega)$ for significant wave height H_s=1 m for North-East Atlantic region estimated from data published in (De Hauteclocque et al., 2023).

However, a comparison of frequency-weighted average power generation (19), which integrates the product of the power generation (as per Fig. 5d) and the wave frequency distribution $p_{ss}(\omega)$ for a significant wave height H_s=1 m, (as estimated for the North-East Atlantic ocean region (De Hauteclocque et al., 2023) in Fig. 6), reveals that the average power generated by the 2-body device P_{avr}=4.79 kW is significantly lower than the power generated by the single-body system $\tilde{P}_{avr}$=40.27 kW.

The trade-off between the magnitude of the buoy hull displacement $|X_2|$ and corresponding power generation as a function of the wave frequency ω, for the 2-body WEC, is illustrated in Fig. 7. The traditional (ideal) Fano resonance effect is visible between $1.8 < \omega < 2.7$ rad/s. The magnitude of the buoy is almost 0 (blue line), and the internal translator fluctuates inside the buoy (red line), but power production is relatively insignificant.

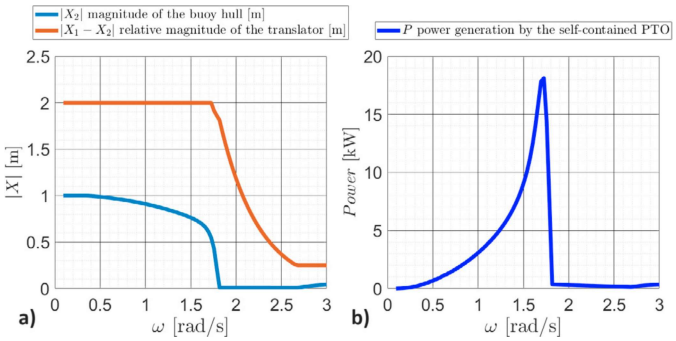

Fig. 7. a) Constrained magnitude for the 2-body buoy hull with dimensions: r=2m, h=4m, and mass m_h=19,132kg with the self contained PTO and b) Corresponding power generation.

Further limitation of the buoy displacement or increase in power generation can be achieved only by adjusting the buoy hull properties Z_{hull} as well as the internal mass m_p value, as will be illustrated in the next example.

5.2 Example 2

The newly selected buoy hull is a cylinder with radius r=4 m, height h=8 m, and mass m_h=153,058 kg. The chosen internal mass m_p=51,019 kg leads to a semi-submerged state for the buoy hull in still water. It is evident that this new cylinder provides significantly more space for the internal mass fluctuation $0.25 < |X_1 - X_2| < 4$ m, as well as accommodating a heavier internal mass m_p, allowing for greater power generation power. The corresponding intrinsic impedance, $Z_{hull}(\omega)$, and excitation force $F_{ex}(\omega)$ frequency responses are illustrated in Fig. 8.

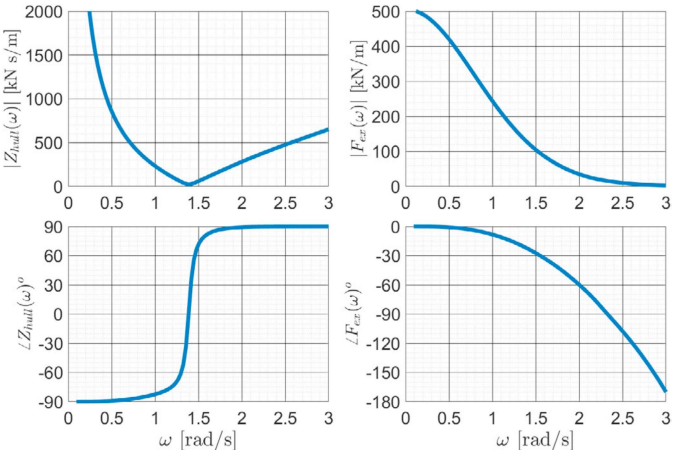

Fig. 8. Intrinsic impedance Z and excitation force F_{ex} frequency responses for the semi-submerged cylindrical buoy hull with dimensions: r=4m, h=8m, and mass m_h=51,019kg, computed using Ansys AQWA (2015)

The solution to the constrained optimization problem $|X_2| < 1$ m, $P(\omega) \to \max$ is presented in Fig. 9. It is clear that the new buoy hull design achieves significant power generation over a larger range of frequencies $\omega > 1$ rad/s (Fig. 9d) compared to the original buoy hull design (Fig. 5d). As a result, the average power generation for the self-contained system $P_{avr} = 73$ kW is now comparable to the average power generation by the ocean bed-based PTO $\tilde{P}_{avr} = 112.2$ kW.

Another method to increase the performance of the 2-body device is to increase the value of the internal mass m_p while reducing the mass of the heaving buoy hull m_h. Thus, in the case when $m_h = m_p = 102kg$, average power generation by the self-contained system $P_{avr} = 103.5$ kW is virtually the same as the power generation by the single-body device at $\tilde{P}_{avr} = 112.2$ kW.

6. CONTROL CO-DESIGN ISSUES

From the results in Section 5, there is clearly a broad design space to be explored for the 2-body device, in terms of the hull dimensions and size of the internal mass. Equally, there is considerable flexibility in the choice of whether some of the 'controller' parameters in (6) are derived from physical (k_p, m_p) or 'virtual' (k_c, m_c) or a mixture of both. The use of physical quantities may be cheaper than the required force rating on the generator to produce the equivalent virtual quantities, but significantly

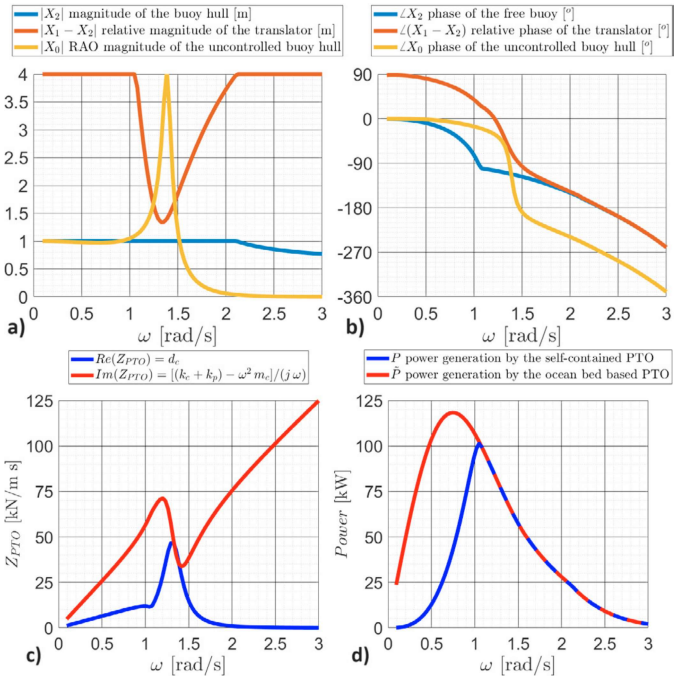

Fig. 9. Optimal constrained control solution for the hull with dimensions: r=4m, h=8m, and mass m_h=51,019kg; a) Magnitudes for the buoy hull and internal translator; b) Corresponding phases; c) Optimal PTO parameters Z_{PTO}; d) Comparison of power generation between the self-contained blue line) and ocean bed-referenced (red line) systems , for identical magnitude constraints (Fig. (a) blue line).

greater flexibility (e.g. real-time adjustment of k_c and m_c) comes with electronic implementation. The relative cost of force and displacement provision in a linear generator is covered, to an extent in (Peña-Sanchez et al., 2022).

This study illustrates that interesting trade-offs exist between the achievable minimum displacement variations and the mean power converted, particularly in relation to a reference single-body device. However, the relatively simple spring/mass/damper controller employed here has limitations in relation to the power/displacement trade-off achievable. Specifically, more advanced controllers, such as MPC, or MPC-like (Faedo et al., 2017) can manage hard constrains more effectively, while fully exploiting the dynamical space within the constraints. Such considerations fall within the area of control co-design, in which integrated system/controller design takes place, recognising the the dependency of the optimal device physical characteristics on the control strategy employed. Some of these issues are usefully addressed for single-body and 2-body system in (Liu et al., 2024).

7. CONCLUSION

Lowering body displacement variations in an actively-controlled WEC may bring benefits in reduced mooring forces and simplified hydrodynamic analysis. The concept of Fano resonance suggests that the hull of a 2-body WEC can effectively be used as a *transmitter* of energy, with all PTO components internalised with the WEC hull. There is considerable design freedom to (economically) optimise the system design, considering trade-offs between capital cost (body component sizes), operational cost (reducing mooring forces), and whether control forces exerted by the generator should be augmented (or to what extent) by internal physical spring and mass components. This preliminary study suggests that there is considerable scope for further investigation.

ACKNOWLEDGEMENTS

The authors are grateful to members of the Centre for Ocean Energy Research, Maynooth University, Ireland, Prof. Kush Bubbar from the University of New Brunswick, Canada, and Prof. M. Tribelsky from M.V. Lomonosov Moscow State University for useful discussions.

REFERENCES

Ansys AQWA (2015). *Aqwa Theory Manual*. ANSYS, Inc.

Cummins, W. (1962). The impulse response function and ship motions. *Schiffstechnik*, 9, 101–109.

De Hauteclocque, G., Vitali Maretic, N., and Derbanne, Q. (2023). Hindcast based global wave statistics. *Applied Ocean Research*, 130, 103438.

Faedo, N., Olaya, S., and Ringwood, J.V. (2017). Optimal control, MPC and MPC-like algorithms for wave energy systems: An overview. *IFAC Journal of Systems and Control*, 1, 37–56.

Falnes, J. (2002). *Ocean Waves and Oscillating Systems: Linear Interactions Including Wave-Energy Extraction*. Cambridge University Press.

Fusco, F. and Ringwood, J.V. (2013). A simple and effective real-time controller for wave energy converters. *IEEE Transactions on Sustainable Energy*, 4(1), 21–30.

Guo, B. and Ringwood, J.V. (2021). Non-linear modeling of a vibro-impact wave energy converter. *IEEE Transactions on Sustainable Energy*, 12(1), 492–500.

Hansen, R.H. (2013). *Design and control of the power take-off system for a wave energy converter with multiple absorbers*. Ph.D. thesis, Department of Energy Technology, Aalborg University.

Lee, C.L., Chen, Y.T., Chung, L.L., and Wang, Y.P. (2006). Optimal design theories and applications of tuned mass dampers. *Eng. Structures*, 28(1), 43–53.

Liu, J., Li, X., Yang, L., Wu, X., Huang, J., Mi, J., and Zuo, L. (2024). Achieving optimum power extraction of wave energy converters through tunable mechanical components. *Energy*, 130322.

Peña-Sanchez, Y., García-Violini, D., and Ringwood, J.V. (2022). Control co-design of power take-off parameters for wave energy systems. *IFAC-PapersOnLine*, 55(27), 311–316.

Rabinovich, M.I. and Trubetskov, D.I. (1989). *Oscillations and Waves in Linear and Nonlinear Systems*. Kluver Academic Publishers.

Ringwood, J.V., Zhan, S., and Faedo, N. (2023). Empowering wave energy with control technology: Possibilities and pitfalls. *Annual Reviews in Control*, 55, 18–44.

Tribelsky, M.I. (2014). *Linear and Nonlinear Evolution in Time and Space*. Shigemasa Printing, Yamaguchi.

Windt, C., Faedo, N., Penalba, M., Dias, F., and Ringwood, J.V. (2021). Reactive control of wave energy devices–the modelling paradox. *Applied Ocean Research*, 109, 102574.